Precise switching control of liquid crystalline microgears driven by circularly polarized light

Kiminori Ito, Hiroshi Frusawa,* and Masahiro Kimura

Institute for Nanotechnology, Kochi University of Technology, Tosa-Yamada, Kochi 782-8502, Japan.

**frusawa.hiroshi@kochi-tech.ac.jp*

Abstract: Liquid crystalline molecules carrying photopolymerizable end groups absorb photon energy via a two-photon process, enabling the photofabrication of 3D structures. In this work, we prepared microgears with different heights and tooth lengths. These birefringent microgears can be induced to rotate by circularly polarized light. Here, we demonstrate that the use of phase plate for switching between left- and right-handed polarization reverses the optically induced rotation while maintaining the same rotational frequency. Due to the precise switching control, these birefringent microgears have advantages over previous microrotors that are fabricated from non-birefringent light-curing resins.

OCIS codes: (160.3710) Liquid crystals; (220.4610) Optical fabrication; (220.4880) Optomechanics; (350.4855) Optical tweezers or optical manipulation.

References and links

1. R. A. Beth, "Mechanical detection and measurement of the angular momentum of light," Phys. Rev. **50**(2), 115–125 (1936).
2. M. E. J. Friese1, T. A. Nieminen, N. R. Heckenberg, and H. Rubinsztein-Dunlop, "Optical alignment and spinning of laser-trapped microscopic particles," Nature **394**(6691), 348–350 (1998).
3. S. L. Neale, M. P. MacDonald, K. Dholakia, and T. F. Krauss, "All-optical control of microfluidic components using form birefringence," Nature Mat. **4**(7), 530–533 (2005).
4. S. Juodkazis, S. Matsuo, N. Murazawa, I. Hasegawa, and H. Misawa, "High-efficiency optical transfer of torque to a nematic liquid crystal droplet," Appl. Phys. Lett. **82**(26), 4657–4659 (2003).
5. H. F. Gleeson, T. A. Wood, and M. Dickinson, "Laser manipulation in liquid crystals: an approach to microfluidics and micromachines," Phil. Trans. R. Soc. A **364**(1847), 2789–2805 (2006).
6. T. A. Wood, H. F. Gleeson, M. R. Dickinson, and A. J. Wright, "Mechanisms of optical angular momentum transfer to nematic liquid crystalline droplets," Appl. Phys. Lett. **84**(21), 4292–4294 (2004).
7. E. Brasselet, N. Murazawa, S. Juodkazis, and H. Misawa, "Statics and dynamics of radial nematic liquid-crystal droplets manipulated by laser tweezers," Phys. Rev. E **77**(4), 04170401–04170407 (2008).
8. K. Ito and M. Kimura, "Optically induced rotation of microcylinders made of photopolymerizable nematic liquid crystal," Jpn. J. App. Phys. **49**(4), 04020801–04020804 (2010).
9. C. Manzo, D. Paparo, L. Marrucci, and I. Jánossy, "Light-induced rotation of dye-doped liquid crystal droplets," Phys. Rev. E **73**(5), 05170701–05170714 (2006).
10. Y. Yang, P. D. Brimicombe, N. W. Roberts, M. R. Dickinson, M. Osipov, and H. F. Gleeson, "Continuously rotating chiral liquid crystal droplets in a linearly polarized laser trap," Opt. Express **16**(21), 6877–6882 (2008).
11. P. Galajda and P. Ormos, "Complex micromachines produced and driven by light," Appl. Phys. **78**(2), 249–251 (2001).
12. S. Maruo, A. Takaura, and Y. Saito, "Optically driven micropump with a twin spiral microrotor," Opt. Express **17**(21), 18525–18532 (2009).
13. H. Ukita and H. Kawashima, "Optical rotor capable of controlling clockwise and counterclockwise rotation in optical tweezers by displacing the trapping position," Appl. Opt. **49**(10), 1991–1996 (2010).

#160805 - $15.00 USD Received 4 Jan 2012; revised 28 Jan 2012; accepted 30 Jan 2012; published 6 Feb 2012

14. S. Maruo, K. Ikuta, and H. Korogi, "Force-controllable, optically driven micromachines fabricated by single-step two-photon microstereolithography," J. Microelectromech. Syst. **12**(5), 533–539 (2003).
15. L. Angelani, R. Di Leonardo, and G. Ruocco, "Self-starting micromotors in a bacterial bath," Phys. Rev. Lett. **102**(4), 04810401–04810404 (2009).

1. Introduction

Micro-objects are optically rotated by light with inherent angular momentum, including lasers with a helical phase structure (e.g., the Laguerre-Gaussian mode) and circularly polarized light [1-9], because micro-objects can extract the angular momentum of such light due to their absorptive or birefringent optical properties [9]. In 1936, circularly polarized light was shown to transfer both angular and linear momentum to quartz plates used as birefringent materials [1]. Laser tweezers can also be used to rotate liquid crystalline (LC) droplets, birefringent liquid particles that are surrounded by solvents, with circularly polarized light, although the shapes of such birefringent micro-objects have been limited to simple configurations of spheres or cylinders [4-9].

The incident light does not necessarily carry angular momentum for the optical rotations. Yang *et al*. reported that continuous rotation of chiral nematic LC droplets is driven by a linearly polarized light [10]. Another alternative strategy is to use micro-objects that can scatter light in a helical manner [11-13]. The photopolymerization of light-curing resins can create microscopic propellers, which have been demonstrated to rotate efficiently due to helical scattering.

While several types of polymeric microrotors [11-14] have potential as driving components of microfluidic devices, fine optical adjustments, including the change of trapping positions, are required for achieving the rotational reversal [13]. In this letter, we impart birefringence to photopolymerizable resins for more precise switching control of microrotors. Although there have been many fundamental studies on the rotational behaviors of LC droplets, both theoretical and experimental [4-7], their potential as elaborate micromachines remains to be explored [8]. We used photopolymerizable LC materials instead of genuine LC droplets and fabricated microgears of various shapes using two-photon microstereolithography. Our aim was to demonstrate the precise switching control of LC microgears compared with previously reported microrotors [1-14].

2. Materials and methods

Nematic LC materials were prepared by mixing a 4-wt.% solution of photoinitiators (Lucirin TPO, BASF) with a reactive monomer LC (Paliocolor LC242, BASF) as the main component. The materials are transparent to near-infrared light but absorb photon energy via a two-photon process, yielding photopolymerized LC resins. The LC molecules were placed on a glass plate that had been covered in advance with a polyvinyl alcohol (PVA) film and rubbed to align the LC molecules along the rubbing direction, and the orientational order was frozen by photopolymerization [8]. Because the materials change to the nematic phase at $63 - 70$ °C, they were heated to 90 °C just prior to photopolymerization to achieve the LC phase. After photopolymerization, the residual LC monomer was removed by washing with ethyl acetate. Accordingly, we manipulated the fabricated objects surrounded by the ethyl acetate solvent.

Figure 1 shows a typical setup used for both fabrication and manipulation. First, we employed a photofabrication system using a mode-locked Ti:sapphire laser (Spectra Physics, Tsunami) producing near-infrared laser light with a wavelength of 730 nm, instead of UV light. The laser emits ultra-short pulses with a pulse width of 130 fs, a repetition rate of 83 MHz, and an average power of 1 W, making it possible to fabricate structures with high resolution via two-photon adsorption as follows. The focus was steered in the horizontal plane by a pair of galvano-mirrors. A focusing unit was attached to the microscope, enabling one to control the

#160805 - $15.00 USD Received 4 Jan 2012; revised 28 Jan 2012; accepted 30 Jan 2012; published 6 Feb 2012

vertical position of the objective. Three-dimensional (3D) photopolymerization was conducted by repeating the above processes. Programmed control of the focusing position allowed for a variety of fabricated micro-objects. To observe the 3D microstructures using scanning electron microscope (SEM: VE-7800, Keyence), the micro-objects were Au-coated, and an acceleration voltage of 10 kV was applied.

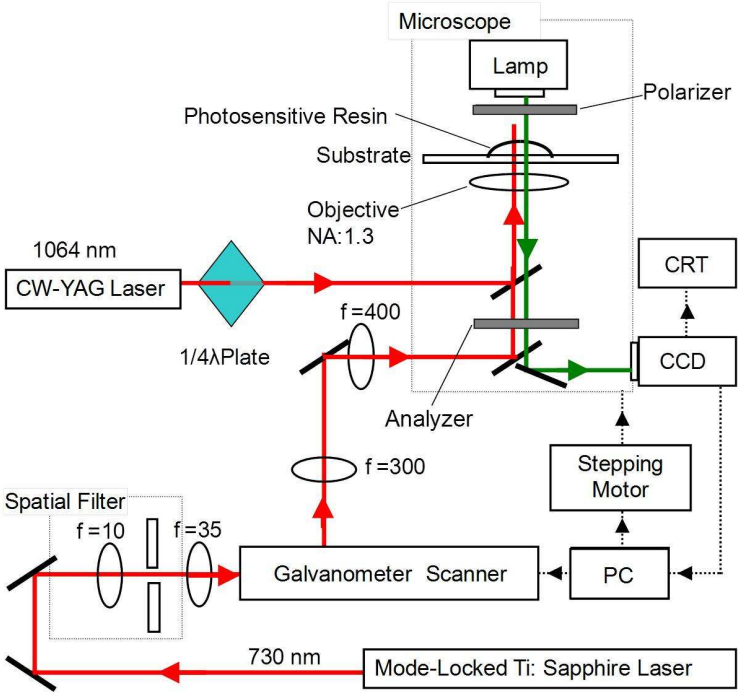

Fig. 1. Schematic diagram of the experimental set-up for optical fabrication and manipulation.

The optical manipulations were performed using a linearly polarized cw Nd:YAG laser ($\lambda = 1064\,\mathrm{nm}$). To trap the LC objects with a circularly polarized beam, a quarter-wave plate was placed in front of the objective lens (NA $= 1.3$). The principal axis of the phase plate had an offset angle of $\pi/4$ with respect to the incident linear polarization direction, producing circular polarization from linearly polarized light. Further rotation of the plate by $\pi/2$ switches between right- and left-handed circularly polarized light. A fast CMOS camera (PL-A741, Pixelink) was equipped with a linear polarization analyzer whose direction was perpendicular to the linear polarization plate, and images were recorded using the crossed Nicols method. Because the micro-objects are birefringent, the intensity of light transmitted through the polarizer has a period of $\pi/2$ with respect to the angle between the polarizer and the fast axis of the birefringent sample. Therefore, we determined the rotational frequencies by detecting the periodically modulated intensities of transmitted light via the aforementioned camera.

3. Results and discussion

3.1. Resolution in fabrication

We measured both the widths and depths of the photofabricated lines using SEM, from which the lateral and vertical resolutions of the present LC resin were evaluated. As the scanning speed of the focal point, v_s, decreases, the occurrence probability of two-photon adsorption increases,

#160805 - $15.00 USD Received 4 Jan 2012; revised 28 Jan 2012; accepted 30 Jan 2012; published 6 Feb 2012

resulting in a varying degree of photopolymerization. We thus adopted both v_s and the light intensity I as photopolymerization parameters. For I ranging from 5 mW to 12.5 mW, v_s was in the range of $48\,\mu\mathrm{m}/s$ to $48\times 9\,\mu\mathrm{m}/s$. We explored a set of optimal parameters, v_s and I, for the present system. Consequently, we found the optimal parameter set of $v_s = 48\times 9\,\mu\mathrm{m/s}$ and $I = 7.5\,\mathrm{mW}$, providing lines that are approximately 180 nm wide and 320 nm high. We used these parameters to photofabricate the LC resins into 3D structures with a resolution that is comparable to that obtained for conventional light-curing polymers [14].

We fabricated four kinds of microgears with different heights and/or tooth lengths. The corresponding SEM images are displayed in Fig. 2. Both of the microgears shown in Fig. 2 have a height h of $h = 10\,\mu\mathrm{m}$, with different tooth lengths. Whereas Fig. 2(a) shows a microgear with a tooth length of 1 μm and a total radius r of $r = 4\,\mu\mathrm{m}$, the microgear in Fig. 2(b) has a tooth length of 2 μm with a core identical to that of Fig. 2(a), giving $r = 5\,\mu\mathrm{m}$. When the microgears were manipulated via optical tweezers, we also used the same type of cross-section, with a different height of $h = 14\,\mu\mathrm{m}$. The aforementioned resolution enables the fabrication that produces the dimensional differences between these four types of 3D structures.

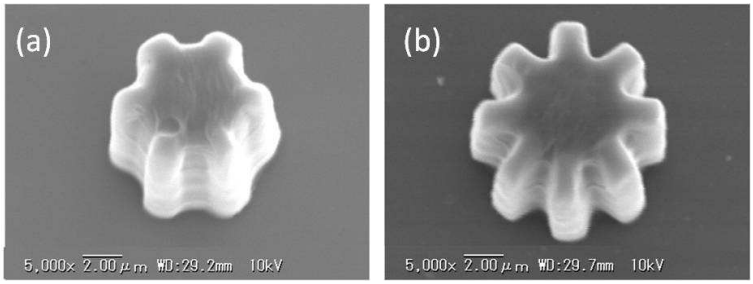

Fig. 2. Scanning electron microscope images of microgears with tooth lengths of 1 μm (a) and 2 μm (b).

3.2. Optically driven rotation

Figure 3 shows the rotational frequencies, f_4^i and f_5^i ($i = t, s$), as a function of beam power at the focal point, where the subscripts of 4 and 5 indicate the radii and the superscripts of t and s indicate, respectively, the heights of the larger ($h = 14\,\mu\mathrm{m}$) and smaller ($h = 10\,\mu\mathrm{m}$) microgears. The red and blue circles in Fig. 3(a), respectively, correspond to f_4^t and f_4^s of the microgears with shorter teeth ($r = 4\,\mu\mathrm{m}$), whereas the same symbols in Fig. 3(b) respectively represent f_5^t and f_5^s of the microgears with longer teeth ($r = 5\,\mu\mathrm{m}$). We see from these data that the rotational frequencies of the microgears are proportional to the laser power, in agreement with previous results for cylindrical shapes [8]. Below, we will discuss three kinds of differences between the slopes: directional changes in rotating the same object, rotation rate differences ($f_4^t > f_4^s$ and $f_5^t > f_5^s$) encountered while increasing the height of microgears with the same tooth length (or the same total radius), and decreasing rotational frequencies ($f_4^t > f_5^t$ and $f_4^s > f_5^s$) caused by extending the teeth of microgears with the same height.

Before comparing the slopes, we present two equations relating to the optical torque Γ resulting from the exchange of momentum between the circularly polarized light and the microgear. First, regarding the incident light, Γ depends on the microgear height h as follows [6]:

$$\Gamma \propto E_0^2 \left\{ 1 - \cos\left(\frac{2\pi}{\lambda} \Delta n h \right) \right\}, \tag{1}$$

where E_0 is the amplitude of the electric field component of the incident light, and Δn is the birefringence. The optical torque Γ is balanced by a viscous drag torque that is exerted on a

#160805 - $15.00 USD Received 4 Jan 2012; revised 28 Jan 2012; accepted 30 Jan 2012; published 6 Feb 2012

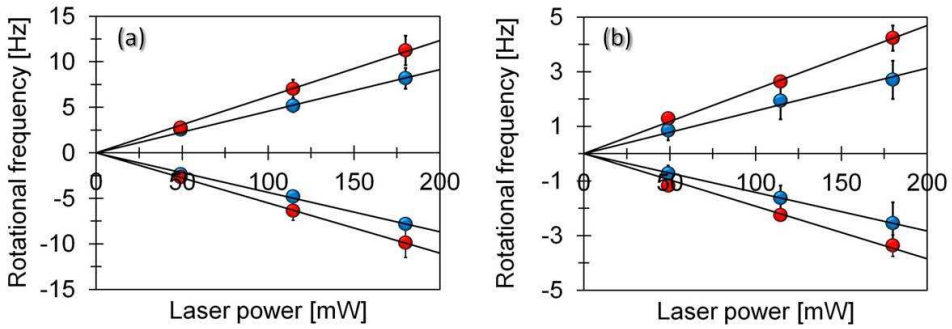

Fig. 3. Dependences of rotational frequency on incident laser power regarding four types of microgears with tooth lengths of 1 μm (a) and 2 μm (b). Red and blue circles represent frequencies for 14- and 10-μm-high microgears, respectively.

disk having a drag coefficient of $(32/3)\eta r^3$ in the overdamped limit [14, 15]:

$$\Gamma = \frac{32}{3}\eta r^3 \Omega, \tag{2}$$

where η is the viscosity of the surrounding solvent, r is the radius of the disk, and $\Omega/2\pi = f$ corresponds to the rotational frequency. It has been found that microgears can be mimicked by disks when the mean radius of $r_m \equiv (r + r_{\rm in})/2$ is used in eq. (2) for evaluating the drag torque [15], where r is the total radius including the teeth and $r_{\rm in}$ is the core radius without the teeth. Equations (1) and (2) imply that the rotational frequencies ($\Omega/2\pi$ in eq. (2)) are proportional to the intensity of the incident light (E_0^2 in eq. (1)), which is validated from Fig. 3.

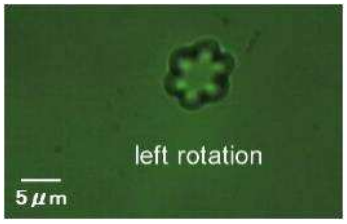

Fig. 4. (Media 1) An optical microsopy image of a microgear ($r = 4\,\mu$m, $h = 14\,\mu$m) which first rotates left and subsequently right by the control of phase plate.

In Fig. 4 (Media 1), we have demonstrated that the LC microgears allow for directional control of optical rotation with the maximum frequency of approximately 11 Hz at a laser power of 180 mW, revealing the superiority of LC micromachines over conventional ones in terms of switching efficiency. In Figs. 3(a) and 3(b), the data points are fitted by two straight lines with opposite slopes, due to switching between left- and right-handed circular polarization of the incident light. A comparison of these slopes shows that the respective differences between the absolute frequency values for the left- and right-handed rotation of the microgears are below 10% and within the error of each data point. The coincidence of rotational frequencies upon a direction reversal validates the mirror symmetry of the exerted torque due to left- and right-handed circularly polarized light. The present reversal requires only the $\pi/2$ rotation of the phase plate, which is an advantage over optically driven micromachines consisting of non-birefringent resins [13, 14].

#160805 - $15.00 USD Received 4 Jan 2012; revised 28 Jan 2012; accepted 30 Jan 2012; published 6 Feb 2012

Figures 3(a) and 3(b) also show that the absolute values of the slopes are greater for the taller microgears with the height of $h = 14\,\mu$m. The optical torque varies with the height h of the microgears, as shown in eq. (1), whereas the drag coefficient given by eq. (2) should be independent of h. Therefore, the present slope difference is associated with the phase angle $\phi(h) = (2\pi/\lambda)h\Delta n$ in the cosine term of eq. (1), as is true for cylindrical objects made of the same LC resin [8]. From the microcylinder results, we found that $\Delta n = 0.12$ [8], which is in agreement with previous evaluations [9]. We can insert the above value of Δn into $\phi(h)$ in addition to $\lambda = 1064$nm, yielding $\phi(10) \approx 2.26\pi$ and $\phi(14) \approx 3.16\pi$. Equation (1) indicates that the phase shift from $\phi(10)$ to $\phi(14)$ in the cosine term creates the variation of optical torque, explaining the slope difference caused by the height variation.

Finally, we evaluated the optical torque from the balance equation (2) using the viscosity of ethyl acetate ($\eta = 0.423$ mPa s) at 298 K. Table 1 displays the variance of torques at the maximum power (180 mW), which are the averaged results for left- and right-handed circularly polarized light. These values are comparable to the drag torques that have been evaluated for LC droplets without polymerization [6]. Moreover, other rotors, including microturbines and micro-propellers composed of non-LC resins, have also been driven by optical torques of the same order [11, 14]; however, we would like to stress again that the efficient reversal of rotational direction has not been realized for conventional non-LC microgears. A comparison between rotational frequencies, which were evaluated using eq. (2), indicates that the torques on even microgears decrease with increasing radius: $\Gamma_5^t/\Gamma_4^t \approx 0.5$ and $\Gamma_5^s/\Gamma_4^s \approx 0.5$, even for the same incident light intensity, where the subscripts and superscripts of Γ are the same as those of the rotational frequencies, such as f_5^i and f_4^i ($i = t, s$). It should be noted that the extent of torque reduction due to decreasing microgear radius is in agreement with that of LC droplets having similar radii [6]. This consistent reduction implies that the transfer of angular momentum to the LC material includes the light-scattering process [6, 9], which should depend on the object size.

Table 1. Mean rotational frequencies and torques at a laser power of 180 mW.

Microgear type		**Mean frequency** [$\times 10^1$ Hz]	**Mean torque** [$\times 10^1$ pN μm]
r [μm]	h [μm]		
4	14	1.1 ± 0.16	1.3 ± 0.19
	10	0.8 ± 0.1	1 ± 0.1
5	14	0.4 ± 0.04	0.7 ± 0.07
	10	0.3 ± 0.05	0.5 ± 0.09

4. Conclusion

We have shown that LC microgears are promising as rotary microactuators because circularly polarized light can be used to precisely control both the frequency and direction of the rotation. Possibilities for future work include the fabrication of more complicated structures, such as micro-sprinklers for utilizing centrifugal force due to high-speed rotations, or the application of an external electric field for fixing the internal degree of the LC directors, which would provide more precise control of the LC rotor motion.

#160805 - $15.00 USD Received 4 Jan 2012; revised 28 Jan 2012; accepted 30 Jan 2012; published 6 Feb 2012